Rapid Communications

## Josephson radiation from nonlinear dynamics of Majorana zero modes

Jia-Jin Feng, <sup>1,2,\*</sup> Zhao Huang <sup>0,3,4,\*</sup> Zhi Wang <sup>0,1,†</sup> and Qian Niu<sup>5</sup>

<sup>1</sup>School of Physics, Sun Yat-sen University, Guangzhou 510275, China

<sup>2</sup>International Center for Quantum Materials, Peking University, Beijing 100871, China

<sup>3</sup>Theoretical Division, Los Alamos National Laboratory, Los Alamos, New Mexico 87545, USA

<sup>4</sup>Texas Center for Superconductivity, University of Houston, Houston, Texas 77204, USA

<sup>5</sup>Department of Physics, The University of Texas at Austin, Austin, Texas 78712, USA

(Received 2 December 2019; revised manuscript received 17 March 2020; accepted 20 April 2020; published 7 May 2020)

Josephson radiation is a powerful method to probe Majorana zero modes in topological superconductors. Recently, Josephson radiation with half the Josephson frequency has been experimentally observed in a HgTe-based junction, possibly from Majorana zero modes. However, this radiation vanishes above a critical voltage, sharply contradicting previous theoretical results. In this Rapid Communication, we theoretically obtain a radiation spectrum quantitatively in agreement with the experiment after including the nonlinear dynamics of the Majorana states into a standard resistively shunted junction model. We further predict two alternative structures of the radiation spectrum for future experimental verification: an interrupted emission line and a chaotic regime. We develop a fixed-point analysis to understand all these features. Our results resolve an apparent discrepancy between theory and experiments, and will inspire the reexamination of structures in radiation spectra of various topological Josephson junctions.

DOI: 10.1103/PhysRevB.101.180504

The fault-tolerant quantum storage and operation is one of the promising schemes for achieving quantum computation [1]. It is based on the premises of non-Abelian statistics, which is associated with the Majorana zero modes in topological superconductors [2]. Identifying the Majorana zero modes in realistic experimental setups remains a challenge [3]. Among various methods [4–6], the Josephson effect has attracted considerable attention due to its phase-sensitive nature [7-20]. The Majorana zero modes in a Josephson junction carry a nontrivial Josephson current with  $4\pi$  periodicity in the Josephson phase [21,22], which is in contrast to the  $2\pi$ -periodic Josephson current in conventional junctions. However, its direct measurement is hindered by the coupling to other distant Majorana zero modes or other quasiparticle excitations [23–26]. The hybridization opens a small gap in the  $4\pi$ -periodic Andreev levels and breaks the local parity conservation [23], reducing the  $4\pi$  periodicity to  $2\pi$ periodicity.

To circumvent this difficulty one can drive nonequilibrium dynamics with a timescale shorter than the equilibration time [27–36], extracting  $4\pi$ -periodic information from the electromagnetic radiation of the junction [13,15,17]. An extra emission line in the spectrum function with half of the Josephson frequency  $f_1/2$  was expected as a result of the  $4\pi$ -periodic Josephson relation from Majorana zero modes [33], as illustrated in Fig. 1(a). In a recent experiment [13], this emission line was indeed observed in a HgTe-based topological junction. However, it mysteriously vanishes above a

critical voltage, which is inconsistent with previous theories on the Josephson radiation [13]. This discrepancy endangers the claim of the Majorana zero modes in such topological junctions.

In this Rapid Communication, we reveal that the Josephson radiation spectra found in the experiments can be well explained after considering the correlation between the nonlinear dynamics of the Josephson phase and the time evolution of Majorana states [37]. By including the Majorana states into the standard resistively shunted junction model, we show that this correlation induces an exact cancellation of the  $4\pi$ -periodic Josephson current for voltages above a critical value, which leads to the vanishment of  $f_{\rm I}/2$  radiation. In particular, our results show a quantitative agreement with the experimental data. For a better understanding, we cast the model into an equivalent classical model with three nonlinear equations, and use the method of averaging to obtain the fixed-point portrait. We find that the vanishment of the emission line can be well characterized by behaviors of the fixed points. We also predict different interrupted emission lines and chaotic dynamics in parameter regimes not yet experimentally explored. Our results highlight the rich physics stemming from the interplay between nonlinear dynamics and nontrivial topology in quantum materials.

Superposition of Majorana states with opposite parities. Before theoretically demonstrating the vanishment of the emission line with the frequency  $f_1/2$ , we first come to the conventional wisdom for the analysis of Josephson radiation from the  $4\pi$ -periodic Josephson effect, and see its limitations in explaining the existing experiments.

For a topological Josephson junction, it is well known that the Majorana zero modes carry the Josephson

<sup>\*</sup>These authors contributed equally to this work.

<sup>†</sup>wangzh356@mail.sysu.edu.cn

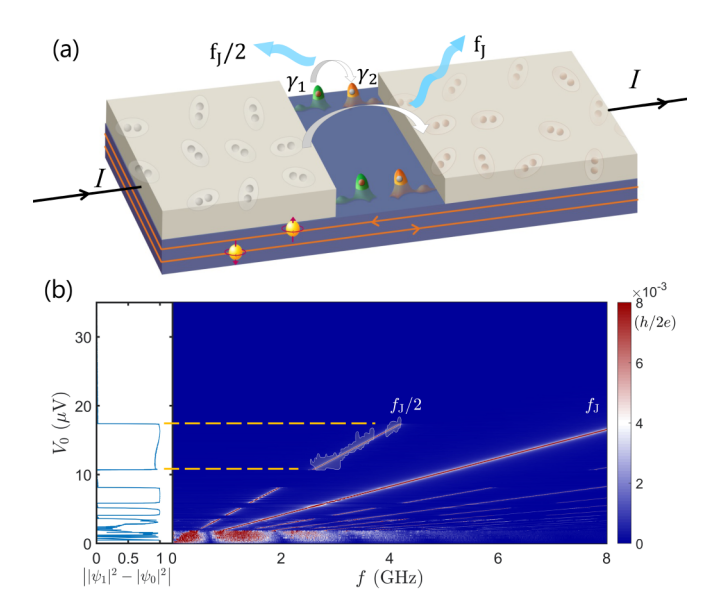


FIG. 1. (a) Schematic setup for Josephson radiation from an overdamped junction with Majorana zero modes. The junction is formed by two ordinary s-wave superconductors (gray) on top of a quantum-spin-Hall insulator (blue), whose edge states host four Majorana zero modes. Cooper-pair tunneling emits Josephson radiation with a quantized frequency  $f_{\rm J}=2eV/h$ , while the singleelectron tunneling through Majorana zero modes emits radiation with half frequency  $f_{\rm J}/2$ . (b) Radiation spectra from the numerical simulations of a quantum resistively shunted junction model. The  $f_1/2$  emission line vanishes above a critical voltage, in agreement with recent experimental results (gray patch). The appearance of the  $f_{\rm J}/2$  line corresponds to the nonzero expectation value  $|\psi_1|^2 - |\psi_0|^2$ of the two-level system from Majorana zero modes, as illustrated on the left. Parameters are  $E_{\rm M}=19.6~\mu{\rm eV},\,\delta=0.196~\mu{\rm eV},\,R=50~\Omega,$  $I_{\rm M}=16$  nA, and  $I_{\rm J}=63$  nA in Eqs. (2) and (3), which are realistic values close to the estimations in the experiment [13]. We scan  $I_{\text{in}} \in [0, 0.7 \ \mu\text{A}]$  to obtain radiation spectra for  $V_0 \in [0, 35 \ \mu\text{V}]$ .

current [21,23] with a  $4\pi$ -periodic current-phase relation  $I \propto \pm \sin \theta / 2$ , where  $\theta$  is the Josephson phase and the plus/minus sign represents the fermionic parity defined by the two Majorana zero modes. If we consider a dc voltage  $V_0$ , the Josephson phase increases linearly with time according to the ac Josephson relation  $\theta(t) = 2eV_0t/\hbar$ , and leads to  $I \propto \pm \sin eV_0 t/\hbar$ , which induces electromagnetic radiation with a frequency of  $eV_0/h$ . It is exactly half of the conventional quantized Josephson frequency  $f_{\rm J}=2eV_0/h$ . Pictures may become even clearer from a quantum point of view. The radiation with frequency  $f_{\rm J}$  represents the energy loss for a Cooper pair to tunnel through a junction biased with voltage  $V_0$ , while the radiation with frequency  $f_{\rm J}/2$  corresponds to the coherent single-electron tunneling through the Majorana channel, as illustrated in Fig. 1(a). It is important to see that whichever picture we take, the  $f_{\rm J}/2$  radiation is predicted to exist for all voltages by the theory, which thus cannot explain its vanishment above a critical voltage in the recent experiment.

The central idea of solving this discrepancy lies at the plus/minus sign in front of the current-phase relation. At first glance, one can take either sign since the radiation spectra are identical. A more careful examination, however, brings to light a key observation that the sign itself can

be time dependent, and correlate with the dynamics of the Josephson phase, possibly causing a dramatic modification of the radiation spectra. To correctly take this phenomenon into consideration, the fermionic parity of the Majorana zero modes must be examined in more detail. The two Majorana zero modes  $\gamma_1$  and  $\gamma_2$  define a parity operator  $\hat{s}_z = i\gamma_1\gamma_2$  which has two eigenstates,  $\hat{s}_z|0\rangle = -|0\rangle$  and  $\hat{s}_z|1\rangle = |1\rangle$ . In the junction these two states constitute a typical two-level system and the system can stay at the superposition state  $|\psi\rangle = \psi_0|0\rangle + \psi_1|1\rangle$ . The supercurrent through the Majorana zero modes should be determined by the expectation value of the parity operator [23,37]

$$I = I_{\mathcal{M}} \langle \psi | \hat{s}_z | \psi \rangle \sin(eV_0 t/\hbar), \tag{1}$$

with  $\langle \psi | \hat{s}_z | \psi \rangle = |\psi_1|^2 - |\psi_0|^2$ .

Now the physics is clear. If  $|\psi\rangle$  stays on the eigenstate  $|0\rangle$  or  $|1\rangle$ , we have  $\langle\psi|\hat{s}_z|\psi\rangle=\pm 1$  and the  $4\pi$ -periodic emission line exists for all voltages, which contradicts the experimental results. However, if  $|\psi\rangle$  is a superposition state with  $|\psi_0|=|\psi_1|$ , we have  $\langle\psi|\hat{s}_z|\psi\rangle=0$ , which means zero current through the Majorana channel. As we will see in the following, the equal superposition state is indeed the case for high voltage due to the correlation between the nonlinear dynamics of the Josephson phase and the time evolution of hybridized Majorana states. This naturally explains the experimentally observed vanishment of the  $4\pi$ -periodic radiation.

Numerical simulation of experimental observation. The complete model for the dynamics in this junction requires the inclusion of a dynamical equation for the two-level system. This has been established in a quantum resistively shunted junction model [37,38]. For a HgTe-based junction, a minimal model requires two ordinary s-wave superconductors on top of a quantum-spin-Hall insulator [23], as shown in Fig. 1(a). When we consider the total parity conservation [37,39], we can obtain the Schrödinger equation for the two-level system as

$$i\hbar \frac{d}{dt} \begin{pmatrix} \psi_0 \\ \psi_1 \end{pmatrix} = \begin{pmatrix} E_{\rm M} \cos \frac{\theta}{2} & \delta \\ \delta & -E_{\rm M} \cos \frac{\theta}{2} \end{pmatrix} \begin{pmatrix} \psi_0 \\ \psi_1 \end{pmatrix},$$
 (2)

where  $E_{\rm M}$  represents the Josephson energy from the coupling between the Majorana zero modes at the left and right interface, and  $\delta$  is the hybridization energy from the wave-function overlap between the Majorana zero modes at the upper and lower edge in Fig. 1(a) [39]. We notice that the Josephson phase  $\theta$  is a variable of the Hamiltonian of the two-level system, meaning that the Josephson phase dynamics directly influences the evolution of the wave function. The Hamiltonian in Eq. (2) is originally derived when a ferromagnet was introduced to break the time-reversal symmetry [23]. The experiment, however, is performed on a junction where time-reversal symmetry is not explicitly broken by a ferromagnet or a magnetic field [13]. Among the theoretical mechanisms for explaining this issue [39-42], we adopt the implicit time-reversal symmetry breaking picture [13], and build our minimal model based on the experimental facts of the existing  $f_{\rm I}/2$  radiation.

By solving the Schrödinger equation, we can obtain the Josephson current carried by the Majorana zero modes. Adding this tunneling current to the resistively shunted

junction equation [43], we arrive at the dynamical equation for the Josephson phase,

$$\dot{\theta} = \frac{2eR}{\hbar} \left[ I_{\rm in} - I_{\rm J} \sin \theta - I_{\rm M} (|\psi_1|^2 - |\psi_0|^2) \sin \frac{\theta}{2} \right], \quad (3)$$

where R is the resistance of the junction,  $I_{\rm in}$  is the injected current,  $I_{\rm J}$  represents the maximum  $2\pi$ -periodic supercurrent from the Cooper-pair tunneling [44], and  $I_{\rm M}$  represents the maximum  $4\pi$ -periodic supercurrent from the single charge tunneling through Majorana zero modes. Equations (2) and (3) couple the Josephson phase  $\theta$  and the Majorana state  $|\psi\rangle$ , and must be solved simultaneously to obtain the full dynamics of the junction. This is a minimal model for studying the dynamics of the topological Josephson junctions. It can be interpreted as equations of motion for a particle with a pseudospin- $\frac{1}{2}$ , subject to a one-dimensional spin-dependent potential. This model has been used to successfully explain the nontrivial hysteretic I-V curves in topological Josephson junctions [37].

The analysis of radiation spectra is based on the solution of Eqs. (2) and (3). Upon the injected current  $I_{\rm in}$  being larger than the critical current, the Josephson phase begins to increase with an oscillating velocity, which induces both dc and ac voltage by checking  $V(t) = \hbar \dot{\theta}(t)/2e$ . The dc voltage pumps in energy and the ac voltage emits electromagnetic energy. Numerically, we take a Fourier transformation to obtain the spectrum function  $v(f, I_{\rm in}) = \frac{1}{T} \int_0^T V(t, I_{\rm in}) e^{-i2\pi f t} dt$  by sweeping the values of f and  $I_{\rm in}$ . Here, the zero-frequency spectrum function is the dc voltage  $V_0 \equiv v(f=0, I_{\rm in})$ . We then rewrite the finite frequency spectrum as a function of frequency and dc voltage  $v(f, V_0)$  to compare with experiments. When  $|\psi_1|^2 - |\psi_0|^2$  is fixed and nonzero, we can analytically obtain  $V(t) = \sum_n v(nf_{\rm J}/2)e^{i2\pi nf_{\rm J}/2}$  which has quantized frequencies [39].

We have specifically chosen realistic parameters to obtain the emission lines shown in Fig. 1(b). Several straight emission lines are presented, corresponding to the quantized radiation frequencies  $f_J/2$ ,  $f_J$ , and higher harmonics. All the emission lines are sharp and straight, consistent with the quantization feature of the Josephson radiation that appeared in conventional junctions. The surprise comes from the  $f_J/2$  emission line. Our simulation shows a unique feature: The emission line vanishes above a critical voltage.

This unusual feature is highly relevant to recent experimental observations and beyond the limitations of the conventional resistively shunted junction (RSJ) model. As reported in a HgTe-based topological junction in Ref. [13], a clear termination of the  $f_{\rm J}/2$  emission line is observed. The gray patch in Fig. 1(b) is the radiation spectrum observed in the experiment for the  $f_{\rm J}/2$  frequency, which is dragged out from Fig. 2(f) in Ref. [13]. With our realistic parameters, we can repeat this experimental data as shown by the solid line overlapping with the shadow. The correlation between the Josephson phase and the wave function of the Majorana state in the dynamics is crucial for this phenomenon.

Prediction of the interrupted emission line and chaotic dynamics. Besides the successful theoretical duplication of the vanishment of the  $f_{\rm J}/2$  Josephson radiation at high voltages, we further find another phenomenon: The emission

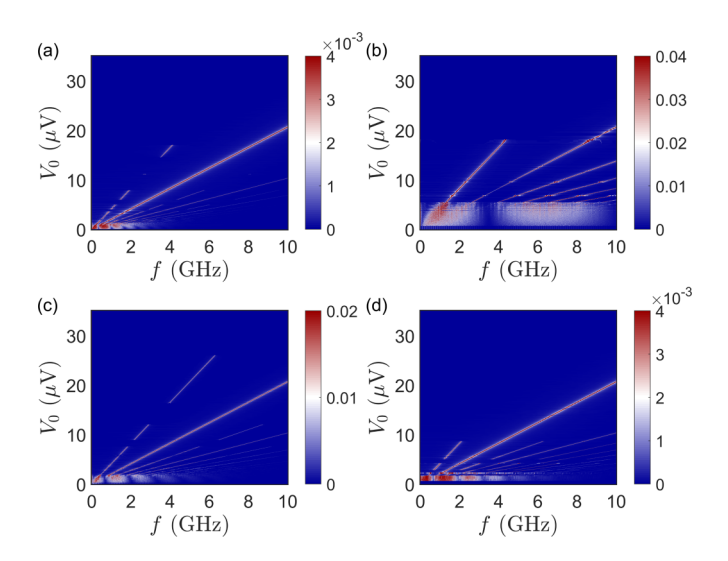


FIG. 2. Radiation spectra from the numerical simulations of the quantum resistively shunted junction model for four typical parameters: (a)  $R/R_0 = 0.5$ , (b)  $R/R_0 = 5$ , (c)  $E_{\rm M}/E_{\rm M0} = 1.5$ , and (d)  $E_{\rm M}/E_{\rm M0} = 0.5$ , where  $R_0$  and  $E_{\rm M0}$  represent the parameters used in Fig. 1(b), while all other parameters are taken the same.

line is interrupted at low voltages. This is especially clear for  $f \in [0, 2 \text{ GHz}]$  in Fig. 1(b). We intentionally changed the background color in this range because it is outside the detection area of the previous experiment [13]. We point out that, in the existing experimental data, there is already some slight discontinuity in the  $f_J/2$  emission line, which might be relevant to our prediction. In the meantime, we also notice interesting chaotic behavior at the zero-voltage limit, shown as noiselike results at the bottom of Fig. 1(b). These chaotic behaviors originate from the nonlinearity in the dynamics. Noticing that noiselike signals already emerge in recent experiments [17], we expect an experimental check in the near future on these predictions.

Now let us explore why the radiation vanishes above the critical voltage and the emission line is interrupted at low voltages. For a nonzero voltage,  $|\psi_1|^2 - |\psi_0|^2$  evolves to a static value if the dynamics is not chaotic. This value as a function of  $V_0$  is shown on the left-hand side of Fig. 1(b). For certain regimes of  $V_0$ , this value becomes zero in this dynamics, which leads to zero tunneling current through the Majorana channel. This is the reason for the vanishment of  $f_{\rm I}/2$  radiation. Outside these regimes, currents from opposite parities do not cancel  $(|\psi_1|^2 - |\psi_0|^2 \neq 0)$ , so we can have the  $f_{\rm J}/2$  emission line. Therefore, we get an interrupted emission line. We can see clearly the quantitative matching between the zero expectation value and the vanishment of the  $f_{\rm J}/2$ emission line. In particular, for the high-voltage limit,  $|\psi_1|^2$  –  $|\psi_0|^2$  is always zero. We thus have a critical voltage above which the emission line is always absent.

Now we investigate how the above features change with experimentally controllable parameters. In Figs. 2(a) and 2(b) we change the resistance to half and ten times the value used in Fig. 1(b). We find that changing the resistance does not influence the critical voltage. However, the interrupted feature is significantly modulated. The reduction of the resistance shortens the emission segments, while increasing

the resistance results in elongation of the segments. For a large resistance, as shown in Fig. 2(b), the segments fuse into a single emission line. In this limit, we can no longer see the interruption. In Figs. 2(c) and 2(d) we modulate the Josephson energy  $E_{\rm M}$  to half and twice the value used in Fig. 1(b). We find that the critical voltage is proportional to the Josephson energy, which is suitable for an experimental check since the Josephson energy can be easily modulated by orders with a gate voltage. These results for different parameters provide detailed guidance to check the structure of the Josephson radiations from the  $4\pi$ -periodic Josephson relation experimentally.

Theoretical understanding based on fixed-point analysis. The key ingredient to our explanation of the vanishing  $f_J/2$  emission line is the damping of the expectation value  $|\psi_1|^2 - |\psi_0|^2$  which causes a perfect cancellation of the  $4\pi$ -periodic supercurrent. This quantum damping can be understood more transparently by casting the quantum resistively shunted junction model into a classical nonlinear model [45–47]. We define  $s_z = |\psi_1|^2 - |\psi_0|^2$  and  $\phi = \arg \psi_1 - \arg \psi_0$ . Equations (2) and (3) are transformed into three classical equations,

$$\dot{\theta} = \frac{1}{\tau_{\theta}} (1 - I_1 \sin \theta - I_2 s_z \sin \theta / 2), \tag{4}$$

$$\dot{\phi} = \frac{1}{\tau_{\phi}} \cos \frac{\theta}{2} + \frac{s_z}{\tau_s \sqrt{1 - s_z^2}} \cos \phi, \tag{5}$$

$$\dot{s}_z = -\frac{1}{\tau_s} \sqrt{1 - s_z^2} \sin \phi, \tag{6}$$

where  $I_1 = I_J/I_{\rm in}$  and  $I_2 = I_M/I_{\rm in}$ . We define three typical timescales  $\tau_{\theta} = \hbar/2eRI_{\rm in}$ ,  $\tau_{\phi} = \hbar/E_{\rm M}$ , and  $\tau_s = \hbar/\delta$ . They determine the scale of velocity for the dynamics of the  $\theta$ ,  $\phi$ , and  $s_z$ , respectively.

This mapping to a pure classical model enables analysis for the dynamics of  $s_z$  through the method of averaging. Since  $\delta$  is exponentially suppressed by the width of the junction and usually very small in the realistic junctions, we can treat  $s_z$  as the slow variable and fix its value to solve Eqs. (4) and (5) first. After obtaining the solution  $\phi(t, s_z)$ , we can then average  $\sin \phi$  over a time period of T with  $\tau_\phi \ll T \ll \tau_s$ , which gives a quantity  $f(s_z) = \frac{1}{T} \int_0^T dt \sin \phi(t, s_z)$ . Plugging it back into Eq. (6), we arrive at a self-consistent equation for the slow variable  $s_z$  as

$$\dot{s}_z = -\frac{f(s_z)}{\tau_s} \sqrt{1 - s_z^2}. (7)$$

This equation determines the phase-space flow for  $s_7$ .

Two typical examples of such flow for the high- and low-voltage regime are shown in Fig. 3(a), where the direction of the phase-space flow is indicated by small arrows. By obtaining the fix points with  $\dot{s}_z = 0$ , we notice a fixed point at  $s_z = 0$  for both cases. For the high-voltage scenario shown as the red-curve, this fixed point is the only stable fixed point, which dominates the whole phase space. Any initial state for  $s_z$  inevitably flows to  $s_z = 0$ . The corresponding time evolution of  $s_z$  is shown as the red curve of Fig. 3(b), which can be analytically described with a damped oscillating evolution as  $s_z(t) \approx e^{-t/\tau_d} \cos(t/\tau_s)$  with  $\tau_d \approx \tau_s \tau_\phi/\tau_\theta$  [37]. For the low-voltage case, however, this fixed point at  $s_z = 0$  becomes an unstable one, which can be easily read out from the reversal of

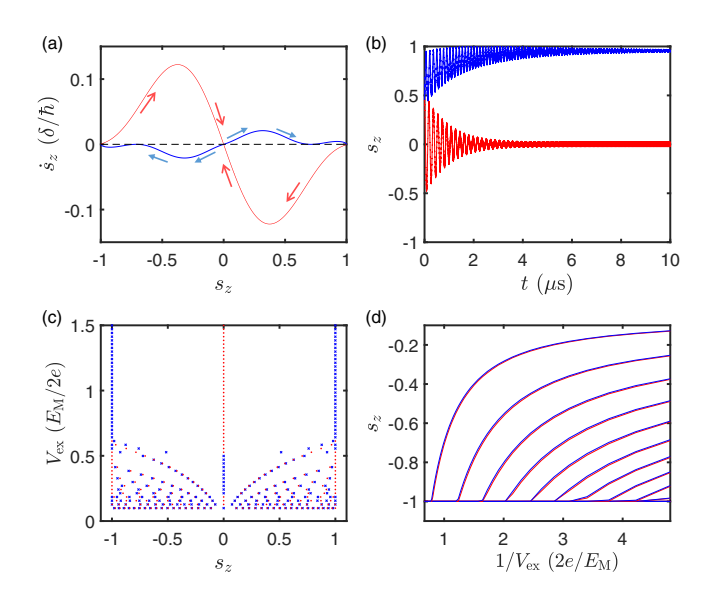


FIG. 3. (a) Phase-space flow for two typical excess voltages  $V_{\rm ex}=0.556E_{\rm M}/2e$  (red curve) and  $V_{\rm ex}=0.498E_{\rm M}/2e$  (blue curve). (b) Time evolution of  $s_z=|\psi_1|^2-|\psi_0|^2$  for the high-voltage case  $V_0=20~\mu{\rm eV}$  (red curve) and the low-voltage case  $V_0=14~\mu{\rm eV}$  (blue curve). (c) Demonstration of stable fixed points (red dots) and unstable fixed points (blue crosses) under the variation of the excess voltages. Other parameters are taken the same as in Fig. 1(b). (d) Illustration of the bifurcation of fixed points with parameters the same as Fig. 2(b).

the flow directions in Fig. 3(a). For this case, the system flows to the stable fixed point at  $s_z \neq 0$ , shown as the blue curve of Fig. 3, then the nonvanishing  $f_J/2$  radiation is expected.

To see the behavior of the phase-space flow more clearly, we demonstrate the portrait of the fixed points as a function of the excess voltage  $V_{\rm ex} \equiv (I_{\rm in} - I_c)R$  in Fig. 3(c), with  $I_c$ the critical current above which the voltage emerges. Let us read this figure from the high-voltage to low-voltage regime. We first find that  $s_z = 0$  is the only stable fixed point at large voltages (red dots). Below a critical excess voltage around  $V_{\rm ex} = 0.5 E_{\rm M}/2e$ ,  $s_z = 0$  changes to an unstable fixed point. The system should flow to other stable fixed points at  $s_z \neq 0$ , which leads to nonvanishing  $f_{\rm J}/2$  radiation. We notice that the fixed point at  $s_z = 0$  switches its stability character multiple times at low voltages, which explains the interrupted line in Fig. 1(b). Another important feature of this fixed-point portrait is the generation of more fixed points when decreasing the voltage. For a clear demonstration, we trace the fixed points with lines and plot them as a function of  $1/V_{\rm ex}$  in Fig. 3(d). We find that the fixed points are generated with a process of splitting one fixed point into three fixed points. This process is known as bifurcation. With decreasing voltage, the bifurcation generates more and more fixed points. When the fixed points become condensed enough that the system could freely wander around the stable ones, the chaotic dynamics naturally emerges. This bifurcation is a standard route towards chaos, and qualitatively explains the noiselike signal at the bottom of Figs. 1(b) and 2.

Conclusion. In summary, we use a quantum resistively shunted junction model to study the Josephson radiation of a topological junction. We find that the  $4\pi$ -periodic Josephson

radiation vanishes above a critical voltage, which explains a recent experiment on HgTe-based topological Josephson junctions. We further predict additional interrupted emission lines and chaotic features in the radiation spectra, which provide guidance for checking the structure of radiation spectra in topological Josephson junctions, and expect their verification by future experiments with a broader parameter range.

Acknowledgments. The authors are grateful to Efstathios G. Charalampidis, Benedikt Fauseweh, James Williams,

Zhong-Bo Yan, and Jianxin Zhu for helpful discussions. This work was supported by NKRDPC-2017YFA0206203, 2017YFA0303302, 2018YFA0305603, NSFC (Grant No. 11774435), and Guangdong Basic and Applied Basic Research Foundation (Grant No. 2019A1515011620). Z.H. is supported by the US DOE Office of Basic Energy Sciences E3B5. Q.N. is supported by DOE (DE-FG03-02ER45958, Division of Materials Science and Engineering), NSF (EFMA-1641101), and the Robert A. Welch Foundation (F-1255).

- [1] A. Yu. Kitaev, Fault-tolerant quantum computation by anyons, Ann. Phys. **303**, 2 (2003).
- [2] J. Alicea, New directions in the pursuit of Majorana fermions in solid state systems, Rep. Prog. Phys. 75, 076501 (2012).
- [3] R. M. Lutchyn, E. P. A. M. Bakkers, L. P. Kouwenhoven, P. Krogstrup, C. M. Marcus, and Y. Oreg, Majorana zero modes in superconductor-semiconductor heterostructures, Nat. Rev. Mater. 3, 52 (2018).
- [4] C. W. J. Beenakker, Search for Majorana fermions in superconductors, Annu. Rev. Condens. Matter Phys. 4, 113 (2013).
- [5] R. Aguado, Majorana quasiparticles in condensed matter, Riv. Nuovo Cimento 40, 523 (2017).
- [6] M. Sato and Y. Ando, Topological superconductors: A review, Rep. Prog. Phys. 80, 076501 (2017).
- [7] Y. Tanaka, T. Yokoyama, and N. Nagaosa, Manipulation of the Majorana Fermion, Andreev Reflection, and Josephson Current on Topological Insulators, Phys. Rev. Lett. 103, 107002 (2009).
- [8] P. A. Ioselevich and M. V. Feigel'man, Anomalous Josephson Current via Majorana Bound States in Topological Insulators, Phys. Rev. Lett. 106, 077003 (2011).
- [9] J. B. Oostinga, L. Maier, P. Schüffelgen, D. Knott, C. Ames, C. Brüne, G. Tkachov, H. Buhmann, and L. W. Molenkamp, Josephson Supercurrent through the Topological Surface States of Strained Bulk HgTe, Phys. Rev. X 3, 021007 (2013).
- [10] P. Matthews, P. Ribeiro, and A. M. García-García, Dissipation in a Simple Model of a Topological Josephson Junction, Phys. Rev. Lett. 112, 247001 (2014).
- [11] B. Sothmann and E. M. Hankiewicz, Fingerprint of topological Andreev bound states in phase-dependent heat transport, Phys. Rev. B 94, 081407(R) (2016).
- [12] Y. Peng, Y. Vinkler-Aviv, P. W. Brouwer, L. I. Glazman, and F. von Oppen, Parity Anomaly and Spin Transmutation in Quantum Spin Hall Josephson Junctions, Phys. Rev. Lett. 117, 267001 (2016).
- [13] R. S. Deacon, J. Wiedenmann, E. Bocquillon, F. Domínguez, T. M. Klapwijk, P. Leubner, C. Brüne, E. M. Hankiewicz, S. Tarucha, K. Ishibashi, H. Buhmann, and L. W. Molenkamp, Josephson Radiation from Gapless Andreev Bound States in HgTe-Based Topological Junctions, Phys. Rev. X 7, 021011 (2017).
- [14] J. Cayao, P. San-Jose, A. M. Black-Schaffer, R. Aguado, and E. Prada, Majorana splitting from critical currents in Josephson junctions, Phys. Rev. B 96, 205425 (2017).
- [15] H. Kamata, R. S. Deacon, S. Matsuo, K. Li, S. Jeppesen, L. Samuelson, H. Q. Xu, K. Ishibashi, and S. Tarucha, Anomalous modulation of Josephson radiation in nanowire-based Josephson junctions, Phys. Rev. B 98, 041302(R) (2018).

- [16] C. Schrade and L. Fu, Parity-Controlled  $2\pi$  Josephson Effect Mediated by Majorana Kramers Pairs, Phys. Rev. Lett. **120**, 267002 (2018).
- [17] D. Laroche, D. Bouman, D. J. van Woerkom, A. Proutski, C. Murthy, D. I. Pikulin, C. Nayak, R. J. J. van Gulik, J. Nygård, P. Krogstrup, L. P. Kouwenhoven, and A. Geresdi, Observation of the 4π-periodic Josephson effect in indium arsenide nanowires, Nat. Commun. 10, 245 (2019).
- [18] H. Ren, F. Pientka, S. Hart, A. T. Pierce, M. Kosowsky, L. Lunczer, R. Schlereth, B. Scharf, E. M. Hankiewicz, L. W. Molenkamp, B. I. Halperin, and A. Yacoby, Topological superconductivity in a phase-controlled Josephson junction, Nature (London) 569, 93 (2019).
- [19] A. Stern and E. Berg, Fractional Josephson Vortices and Braiding of Majorana Zero Modes in Planar Superconductor-Semiconductor Heterostructures, Phys. Rev. Lett. 122, 107701 (2019).
- [20] C. J. Trimble, M. T. Wei, N. F. Q. Yuan, S. S. Kalantre, P. Liu, J. J. Cha, L. Fu, and J. R. Williams, Josephson detection of time reversal symmetry broken superconductivity in SnTe nanowires, arXiv:1907.04199.
- [21] A. Kitaev, Unpaired Majorana fermions in quantum wires, Phys.-Usp. 44, 131 (2001).
- [22] H.-J. Kwon, K. Sengupta, and V. M. Yakovenko, Fractional ac Josephson effect in *p*- and *d*-wave superconductors, Eur. Phys. J. B 37, 349 (2004).
- [23] L. Fu and C. L. Kane, Josephson current and noise at a superconductor/quantum-spin-Hall-insulator/superconductor junction, Phys. Rev. B 79, 161408(R) (2009).
- [24] D. M. Badiane, M. Houzet, and J. S. Meyer, Nonequilibrium Josephson Effect through Helical Edge States, Phys. Rev. Lett. 107, 177002 (2011).
- [25] M. Houzet, J. S. Meyer, D. M. Badiane, and L. I. Glazman, Dynamics of Majorana States in a Topological Josephson Junction, Phys. Rev. Lett. **111**, 046401 (2013).
- [26] F. Crépin and B. Trauzettel, Parity Measurement in Topological Josephson Junctions, Phys. Rev. Lett. **112**, 077002 (2014).
- [27] D. I. Pikulin and Y. V. Nazarov, Phenomenology and dynamics of a Majorana Josephson junction, Phys. Rev. B **86**, 140504(R) (2012).
- [28] P. San-Jose, E. Prada, and R. Aguado, ac Josephson Effect in Finite-Length Nanowire Junctions with Majorana Modes, Phys. Rev. Lett. **108**, 257001 (2012).
- [29] L. P. Rokhinson, X. Liu, and J. K. Furdyna, The fractional a.c. Josephson effect in a semiconductor-superconductor nanowire as a signature of Majorana particles, Nat. Phys. 8, 795 (2012).

- [30] F. Domínguez, F. Hassler, and G. Platero, Dynamical detection of Majorana fermions in current-biased nanowires, Phys. Rev. B 86, 140503(R) (2012).
- [31] J. Wiedenmann, E. Bocquillon, R. S. Deacon, S. Hartinger, O. Herrmann, T. M. Klapwijk, L. Maier, C. Ames, C. Brüne, C. Gould, A. Oiwa, K. Ishibashi, S. Tarucha, H. Buhmann, and L. W. Molenkamp, 4π-periodic Josephson supercurrent in HgTe-based topological Josephson junctions, Nat. Commun. 7, 10303 (2016).
- [32] E. Bocquillon, R. S. Deacon, J. Wiedenmann, P. Leubner, T. M. Klapwijk, C. Brüne, K. Ishibashi, H. Buhmann, and L. W. Molenkamp, Gapless Andreev bound states in the quantum spin Hall insulator HgTe, Nat. Nanotechnol. 12, 137 (2017).
- [33] F. Domínguez, O. Kashuba, E. Bocquillon, J. Wiedenmann, R. S. Deacon, T. M. Klapwijk, G. Platero, L. W. Molenkamp, B. Trauzettel, and E. M. Hankiewicz, Josephson junction dynamics in the presence of 2π- and 4π-periodic supercurrents, Phys. Rev. B 95, 195430 (2017).
- [34] J. Picó-Cortés, F. Domínguez, and G. Platero, Signatures of a  $4\pi$ -periodic supercurrent in the voltage response of capacitively shunted topological Josephson junctions, Phys. Rev. B **96**, 125438 (2017).
- [35] D. Sun and J. Liu, Quench dynamics of the Josephson current in a topological Josephson junction, Phys. Rev. B **97**, 035311 (2018).
- [36] A. Murani, B. Dassonneville, A. Kasumov, J. Basset, M. Ferrier, R. Deblock, S. Guéron, and H. Bouchiat, Microwave Signature of Topological Andreev Level Crossings in a Bismuth-Based Josephson Junction, Phys. Rev. Lett. 122, 076802 (2019).

- [37] J.-J. Feng, Z. Huang, Z. Wang, and Q. Niu, Hysteresis from nonlinear dynamics of Majorana modes in topological Josephson junctions, Phys. Rev. B **98**, 134515 (2018).
- [38] W.-C. Huang, Q.-F. Liang, D.-X. Yao, and Z. Wang, Manipulating the Majorana qubit with Landau-Zener-Stückelberg interference, Phys. Rev. A 92, 012308 (2015).
- [39] See Supplemental Material at http://link.aps.org/supplemental/ 10.1103/PhysRevB.101.180504 for the derivation of the quantum resistively shunted junction model and the numerical details for the Josephson radiation.
- [40] F. Zhang and C. L. Kane, Time-Reversal-Invariant Z<sub>4</sub> Fractional Josephson Effect, Phys. Rev. Lett. **113**, 036401 (2014).
- [41] J. Wang, Y. Meir, and Y. Gefen, Spontaneous Breakdown of Topological Protection in Two Dimensions, Phys. Rev. Lett. **118**, 046801 (2017).
- [42] D. Sticlet, J. D. Sau, and A. Akhmerov, Dissipationenabled fractional Josephson effect, Phys. Rev. B 98, 125124 (2018).
- [43] M. Tinkham, Introduction to Superconductivity (Courier Corporation, North Chelmsford, MA, 2004).
- [44] G. D. Mahan, *Many-Particle Physics* (Plenum, New York, 2000).
- [45] B. Wu and Q. Niu, Nonlinear Landau-Zener tunneling, Phys. Rev. A 61, 023402 (2000).
- [46] J. Liu, L. Fu, B.-Y. Ou, S.-G. Chen, D.-I. Choi, B. Wu, and Q. Niu, Theory of nonlinear Landau-Zener tunneling, Phys. Rev. A 66, 023404 (2002).
- [47] J. Liu, B. Wu, and Q. Niu, Nonlinear Evolution of Quantum States in the Adiabatic Regime, Phys. Rev. Lett. **90**, 170404 (2003).